

Impedances and Instability Studies at the ESR

U. Schaaf, K. Beckert, D. Budicin, H. Eickhoff, B. Franzke
 I. Hofmann, G. Kalisch, F. Nolden, P. Spädtke, M. Steck
 GSI Darmstadt
 P.O.B. 110552
 D-6100 Darmstadt 11

Abstract

Longitudinal and transverse *microwave instabilities* limit beam intensities in heavy ion cooler rings. Intensity thresholds and growth rates of instabilities are mainly determined by longitudinal and transverse *coupling impedances*. These impedances have been evaluated for the ESR by analyzing *beam transfer functions*. Measured longitudinal space charge impedances had values between $Z_{||}/h \approx -i 1000 \Omega$ and $Z_{||}/h \approx -i 1800 \Omega$ whereas transverse space charge impedances varied very strongly between $Z_{\perp} \approx -i 0.9 \text{ G}\Omega/\text{m}$ and $Z_{\perp} \approx -i 16 \text{ G}\Omega/\text{m}$. The impedance of $16 \text{ G}\Omega/\text{m}$ corresponds to a transverse *emittance* of $e = 0.05 \pi \text{ mm mrad}$ and an incoherent *Laslett tune shift* of $\Delta Q_{\text{inc}} = 1.5 \times 10^{-4}$. For the ESR accelerating cavity we found a maximum real impedance of $\text{Re}(Z_{||}/h) = 620 \Omega$ and a resonance width of about 50 kHz [3]. No other strong coupling impedances besides the space charge impedance (and the cavity impedance) have been found in the region below 130 MHz . Maximum longitudinal phase space densities in the ESR were as high as 5.5 times the conventional *Keil-Schnell-threshold*. A similar transverse criterion was exceeded by a factor of 20. With active feedback stabilization, even larger factors are expected in future.

1 INTRODUCTION

In the heavy ion cooler ring ESR, very high phase space densities can be achieved by means of rf-stacking and electron cooling. In the case of a coasting beam, collective plasma oscillations are observed which appear as *longitudinal density waves* and as *transverse dipole waves* travelling along the beam. The reason for the observed collective particle behaviour is the interaction between particles via direct space charge forces or via fields induced in surrounding structures. The strength of this mechanism is described by the longitudinal and transverse *coupling impedances*. These impedances have been evaluated in the ESR by analyzing *beam transfer functions*. As expected for beams with $\gamma \approx 1$, longitudinal and transverse *space charge impedances* dominate over other impedance components. In contrast to the longitudinal space charge impedance, the transverse space charge impedance is very sensitive to variations of the ion beam radius. Measured values differ by more than one order of magnitude whereas longitudinal impedances of electron cooled beams do not change very much. Transverse impedance measurements can therefore be used to evaluate average *beam diameters* and *emittances*.

2 BEAM TRANSFER FUNCTIONS

Taking into account collective effects, the longitudinal beam transfer function is given by the expression [1]

$$\tau_{||} = \frac{\tau_{||}^0}{\epsilon} \quad (1)$$

with the *dielectric function*

$$\epsilon = 1 + Z_{||} \tau_{||}^0 \quad (2)$$

$\tau_{||}^0$ is the familiar transfer function for zero impedance ($\epsilon = 1$) and $Z_{||}$ is the longitudinal coupling impedance with its dominant space charge component

$$Z_{||}^c = -h \frac{iZ_0}{2\beta\gamma^2} [1 + 2 \ln(b/a)] \quad (3)$$

($Z_0 = 377 \Omega$, h : harmonic number of the particle revolution frequency, b : wall chamber radius, a : beam radius). Drawing the inverse transfer function in the complex plane yields the *stability diagram*. From equations 1 and 2 we get

$$\frac{1}{\tau_{||}} = \frac{1}{\tau_{||}^0} + Z_{||} \quad (4)$$

Hence the shift of the stability diagram gives the coupling impedance.

3 SCHOTTKY NOISE

In the case of low phase space densities, the power density $P'(\omega)$ of the Schottky-spectrum gives directly the particle distribution function $\Psi(\omega)$. Taking into account again collective effects, we get

$$P'(\omega) = \frac{\Psi(\omega)}{|\epsilon(\omega)|^2} \quad (5)$$

For cooled low β -beams with high space charge impedance, Schottky-spectra as well as longitudinal beam transfer functions show the well known double peak structure (see fig. 1). The left peak corresponds to a collective density wave travelling slower and the right peak to a wave travelling faster than the average particle velocity.

4 LONGITUDINAL STABILITY DIAGRAM

Figure 2 shows the stability diagram calculated from the transfer function of figure 1 (dashed curve) and the corresponding diagram for zero impedance (diagram which would be measured if the impedance were zero). In addition, also the *Keil-Schnell-circle* is shown. The radius of

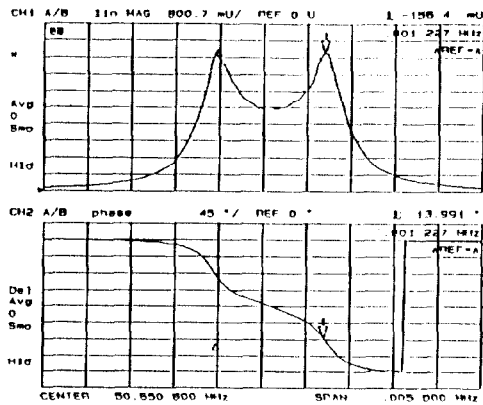


Figure 1: Longitudinal beam transfer function (amplitude and phase) of a cooled $^{40}\text{Ar}^{18+}$ -beam (250 MeV/u, 1.02 mA) at the 30th harmonic.

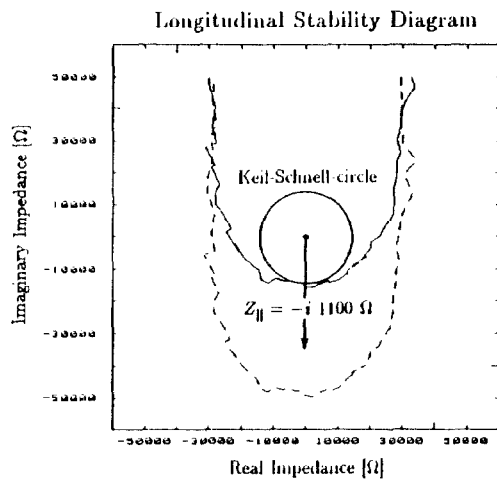


Figure 2: Stability diagram calculated from the transfer function shown in figure 1 (dashed curve) and corresponding diagram for zero impedance.

this circle is given by the distance of the origin to the lower boundary of the zero impedance diagram. The length of the impedance vector is 2.3 times the radius of the Keil-Schnell-circle. For a $^{20}\text{Ne}^{10+}$ -beam (153 MeV/u, 70 μA), the Keil-Schnell-threshold was even exceeded by a factor of 5.5.

5 LONGITUDINAL COUPLING IMPEDANCE

The evaluation of the longitudinal coupling impedance is not straightforward. The problem is to determine the origin of the zero impedance diagram.

For Gaussian distribution functions it can be shown [2] that the zero impedance diagram crosses the imaginary axes at a distance to the origin being 0.7 times the corresponding distance on the real axes. (The shape of measured stability diagrams of electron cooled beams justifies the assumption of a nearly Gaussian distribution function.)

A more general method is to compare the distribution functions calculated from the beam transfer function and

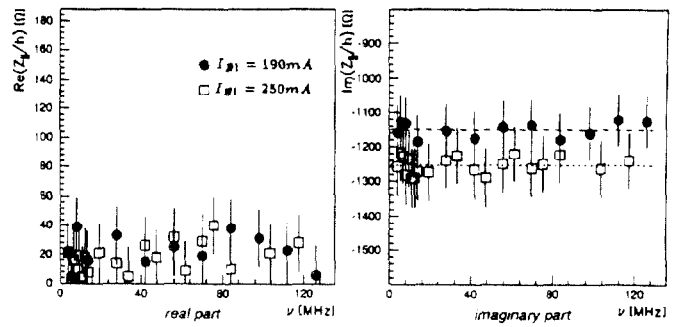


Figure 3: Real part and imaginary part of the longitudinal coupling impedance in a frequency range up to 130 MHz.

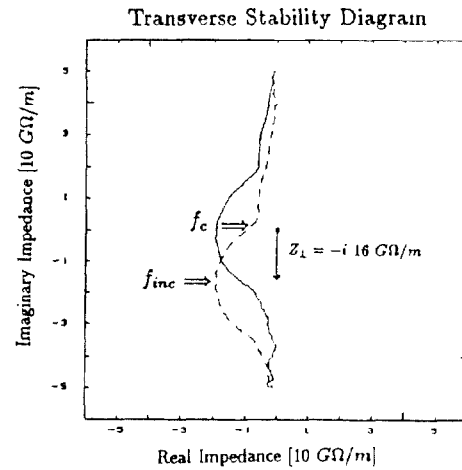


Figure 4: Vertical stability diagram (lower betatron sideband) of a $^{86}\text{Kr}^{36+}$ -beam (152 MeV/u, 20 μA) at the 23rd harmonic.

from the Schottky spectrum for various test impedances. The best estimate for the impedance is found if both distribution functions approach completely.

In both cases the impedances still have to be calibrated. This is done by calculating the zero impedance stability diagram using the uncalibrated impedance. From the zero impedance stability diagram, the particle distribution function can be calculated in a straightforward way. In the next step the distribution function and the impedance are normalized to the beam current (measured with a beam current transformer). Figure 3 shows the measured longitudinal coupling impedance in a frequency range up to 130 MHz. The imaginary part is constant over the entire range as expected for the space charge impedance. For broadband real impedances an upper limit of about $\text{Re}(Z_{||}/h) \leq 40 \Omega$ has been found.

6 TRANSVERSE COUPLING IMPEDANCE

The transverse coupling impedance shifts the transverse stability diagram. Again, the space charge impedance

$$Z_1^{sc} = -\frac{iZ_0C}{2\pi\beta^2\gamma^2} \left[\frac{1}{a^2} - \frac{1}{b^2} \right] \quad (6)$$

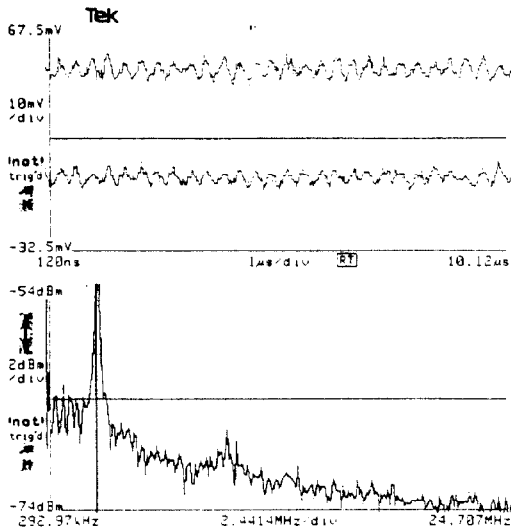


Figure 5: Longitudinal beam instability appearing at the second harmonic of the particle revolution frequency in time domain (upper traces) and frequency domain (lower trace). Beam parameters: ion = $^{20}\text{Ne}^{10+}$, energy = 153 MeV/u, ion current = 1.14 mA.

(C : ring circumference) is the largest component of the total impedance.

Figure 4 shows the vertical stability diagram of a cooled $^{86}\text{Kr}^{36+}$ -beam at the 23rd harmonic. The shift due to the impedance can again be calibrated using the particle distribution function calculated from the zero impedance stability diagram. However, this method only works properly if nonlinear tune shifts can be neglected.

Alternatively, it is possible to evaluate the transverse impedance from the *incoherent Laslett tune shift*

$$\Delta Q_{\text{inc}} = \frac{Z}{A} \frac{I c}{4\pi Q \gamma \omega_0 m_{\text{ion}} c^2 / e} \text{Im} Z_{\perp}, \quad (7)$$

which is calculated from the difference of the coherent betatron frequency f_c and the incoherent betatron frequency f_{inc} (see fig. 4). For the shown example, the results are

$$\begin{aligned} \Delta Q_{\text{inc}} &= 1.5 \times 10^{-4}, \\ \text{Im}(Z_{\perp}) &= -16 \text{ G}\Omega/\text{m}, \\ a &= 1.1 \text{ mm}, \\ e &= a^2/\beta = 0.05 \pi \text{ mm mrad}. \end{aligned}$$

These results have to be compared to a circle approximation for the transverse stability limits (transverse analogy to the longitudinal Keil-Schnell-criterion). With a momentum spread of $\Delta p/p = 2.2 \times 10^{-5}$ we find that this transverse criterion is exceeded by a factor of 20.

7 BEAM INSTABILITIES AND CURES

In the case of high phase space densities, collective waves are travelling along the beam. They can be observed in Schottky-spectra and beam transfer functions (see fig. 1).

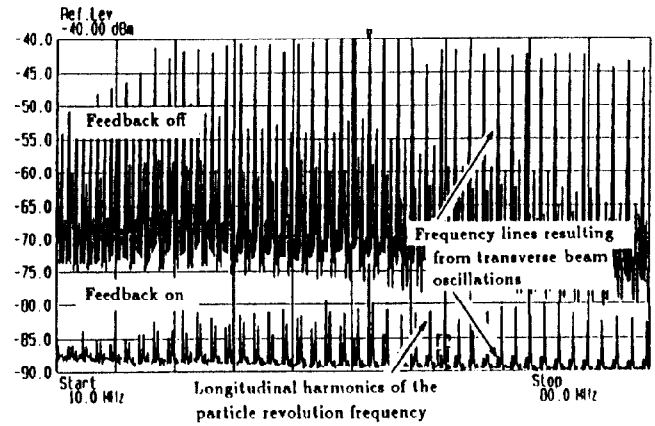


Figure 6: Frequency spectrum of transverse oscillations of a $^{20}\text{Ne}^{10+}$ -beam (153 MeV/u, 3.1 mA) from 10 to 80 MHz with feedback off (upper trace) and feedback on (lower trace).

The beam becomes unstable if at least one of these waves begins to grow exponentially in time.

Figure 5 shows a longitudinal beam instability at the second harmonic of the particle revolution frequency due to the real part of the cavity impedance. The lower part of the picture shows a strong line at the corresponding frequency. In time domain the instability appears as a beam current modulation (upper traces). The instability decreases again because large electromagnetic fields due to the instability change the particle momentum distribution such that beam momentum spread and *Landau damping* are increased.

Whereas longitudinal microwave instabilities only limit the minimum momentum spread of intense cooled beams, transverse instabilities even cause particle losses. At the ESR, transverse dipole instabilities are damped by an active feedback system [2].

Figure 6 shows how large coherent betatron sidebands due to transverse beam oscillations are damped by at least a factor of 10. Simultaneous beam current transformer measurements showed that particle losses disappeared if the feedback was switched on. (Besides the active feedback system, also the *cooling force* of the electron cooler helps to damp transverse as well as longitudinal instabilities [1].) Using active feedback stabilization it should therefore be possible to raise the currents of cooled ESR beams.

8 REFERENCES

- [1] S. Cocher. *Effets Collectifs D'un Faisceau Refroidi D'Ions Lourds Dans Un Anneau De Stockage*, thesis, Université de Paris-Sud, 1989.
- [2] U. Schaaf. *Schottky-Diagnose und BTF-Messungen an gekühlten Strahlen im Schwerionen-Speicherring ESR*, thesis, GSI Report GSI-91-22, 1991.
- [3] G. Kalisch et al. *Longitudinal Space Charge Effects in Cooled Bunched Beams*, these proceedings.